

Effective hydrostatic limits of pressure media for high-pressure crystallographic studies

Ross J. Angel,^{a*} Maciej Bujak,^{a,b} Jing Zhao,^a G. Diego Gatta^c and Steven D. Jacobsen^d

^aCrystallography Laboratory, Department of Geosciences, Virginia Tech, Blacksburg, VA 24060, USA, ^bInstitute of Chemistry, University of Opole, Oleska 48, 45-052 Opole, Poland, ^cDipartimento di Scienze della Terra, Università degli Studi di Milano, Via Botticelli 23, I-20133 Milano, Italy, and ^dDepartment of Earth and Planetary Sciences, Northwestern University, Evanston, IL 60208, USA. Correspondence e-mail: rangel@vt.edu

The behavior of a number of commonly used pressure media, including nitrogen, argon, 2-propanol, a 4:1 methanol–ethanol mixture, glycerol and various grades of silicone oil, has been examined by measuring the X-ray diffraction maxima from quartz single crystals loaded in a diamond-anvil cell with each of these pressure media in turn. In all cases, the onset of non-hydrostatic stresses within the medium is detectable as the broadening of the rocking curves of X-ray diffraction peaks from the single crystals. The onset of broadening of the rocking curves of quartz is detected at ~ 9.8 GPa in a 4:1 mixture of methanol and ethanol and at ~ 4.2 GPa in 2-propanol, essentially at the same pressures as the previously reported hydrostatic limits determined by other techniques. Gigahertz ultrasonic interferometry was also used to detect the onset of the glass transition in 4:1 methanol–ethanol and 16:3:1 methanol–ethanol–water, which were observed to support shear waves above ~ 9.2 and ~ 10.5 GPa, respectively, at 0.8–1.2 GHz. By contrast, peak broadening is first detected at ~ 3 GPa in nitrogen, ~ 1.9 GPa in argon, ~ 1.4 GPa in glycerol and ~ 0.9 GPa in various grades of silicone oil. These pressures, which are significantly lower than hydrostatic limits quoted in the literature, should be considered as the practical maximum limits to the hydrostatic behavior of these pressure media at room temperature.

© 2007 International Union of Crystallography
Printed in Singapore – all rights reserved

1. Introduction

High-pressure crystallographic studies provide a method of probing the repulsive part of the interatomic potential between atoms and between molecules and its influence on molecular packing and bonding. Recent single-crystal studies have revealed, for example, that quite modest pressures lead to new polymorphs in molecular compounds (*e.g.* Allan *et al.*, 2002; Boldyreva *et al.*, 2002) and to changes in bonding in both inorganic compounds (*e.g.* Angel, 1997) and the inorganic components of inorganic–organic hybrid materials (*e.g.* Bujak & Angel, 2006). For many of these studies the 4:1 mixture by volume of methanol and ethanol that has traditionally been used as a hydrostatic pressure medium to pressures slightly in excess of 10 GPa (Piermarini *et al.*, 1973; Eggert *et al.*, 1992; Grocholski & Jeanloz, 2005) is not suitable because it dissolves the samples. Furthermore, these small-molecule alcohols can enter the tunnels or structural cages of some microporous and mesoporous inorganic materials such as zeolites and thereby modify their high-pressure behavior (*e.g.* Hazen, 1983; Hazen & Finger, 1984; Lee *et al.*, 2002). These considerations have

forced the use of a wide range of other media, including condensed gases, water, fluorocarbons and inert silicone oils.

In addition to using a pressure medium that does not dissolve the single-crystal sample, it is also normally desirable to ensure that the stress applied to the sample crystal is homogeneous and that the sample is free of any differential stress or induced shear strain over the entire pressure range of the experiment. To achieve this, the sample must be immersed in a medium that displays hydrostatic behavior. Such a hydrostatic medium cannot, by definition, support shear stresses because it has no shear strength. The motivations for avoiding non-hydrostatic conditions in an experiment are many-fold. From an experimental standpoint, non-hydrostatic stresses create inhomogeneous strain in the crystal and thus broadening of the diffraction peaks from the sample which results in a reduction of the signal-to-noise ratio of the measured diffraction signal. The use of non-hydrostatic pressure media can modify the relative evolution of cell parameters of crystalline samples with pressure (*e.g.* Kenichi, 1999) and can lead to difficulties in characterizing the pressure (and full stress state of the medium) by the commonly used ruby

fluorescence technique (Forman *et al.*, 1972; Sharma & Gupta, 1991; Chai & Brown, 1996) or by an internal diffraction standard. Non-hydrostatic stresses may therefore adversely affect results from equation of state and elasticity studies, especially those aimed at obtaining accurate pressure derivatives of elastic moduli. Furthermore, through coupling to the spontaneous strain, non-hydrostatic stresses can also promote or suppress phase transitions (*e.g.* Decker *et al.*, 1979; Resel *et al.*, 2004) and they can promote the amorphization of crystalline samples (*e.g.* Haines *et al.*, 2001; Machon *et al.*, 2003). In short, the stress state of a non-hydrostatic pressure medium cannot be easily quantified, and the resulting behavior of the sample crystal cannot therefore be related to the experimental conditions.

In the past, limits to the hydrostaticity of pressure media were associated with the onset of line-broadening of the fluorescence spectra of ruby chips immersed in the medium, or with other deviations of the ruby fluorescence spectra from those measured in hydrostatic conditions (Piermarini *et al.*, 1973; Bell & Mao, 1981). However, ruby is a relatively stiff material with a bulk modulus of about 254 GPa (Richet *et al.*, 1988; Kim-Zajonz *et al.*, 1999) and is thus intrinsically less sensitive to non-hydrostatic stresses than most mineral or molecular compounds (Piermarini *et al.*, 1973). Further, the fluorescence spectra are intrinsically broad as a result of defects and strains within the ruby crystals, unless the crystals have been very carefully annealed. Therefore Varga *et al.* (2003) introduced an alternative method of detecting non-hydrostatic stresses in pressure media by following the widths of the diffraction peaks of quartz single crystals. Quartz has the advantage that it is readily available in gem-quality samples that have intrinsically sharp diffraction peaks, it is easy to handle, and it is elastically soft with a bulk modulus of 37.12 (9) GPa (Angel *et al.*, 1997) making the peak positions and widths sensitive to small non-hydrostatic stresses. The results (Varga *et al.*, 2003) obtained by this method for the fluorocarbons known by the trade name 'Fluorinert' have since been confirmed by direct measurements of shear stresses at high pressures (Sidorov & Sadykov, 2005). In this paper we report further observations of line broadening in the diffraction patterns from quartz crystals loaded in a variety of compounds that have been widely used as pressure media in order to provide an indication of their practical hydrostatic limits. To complement these static (X-ray) observations, we also employ a high-frequency (GHz) ultrasonic technique for the diamond-anvil cell (DAC) to investigate the frequency-dependence of the glass transition pressure in methanol-ethanol mixtures.

2. Experimental

For the X-ray diffraction measurements, each pressure medium was loaded into the DAC in turn, along with a quartz test crystal. All of the quartz crystals used were small portions of a single polished 30 μm -thick plate parallel to ($\bar{1}20$). Cryogenic loading under liquid nitrogen was employed for the Ar and N₂ pressure media, during which the DAC was sealed

and pressurized before it was warmed to room temperature for the diffraction measurements. All other media were loaded at room temperature. Anhydrous isopropyl alcohol (dried over a molecular sieve) was obtained from Acros Organics. The two silicone fluids used were hexamethyldisiloxane, C₆H₁₈OSi₂, from Clearco Products Co. Inc., with a reported viscosity of 0.65 cSt, and [CH₃Si(C₆H₅)₂O]₂Si(CH₃)₂ with a reported viscosity of 37 cSt. Glycerol, C₃H₈O₃, of purity 99.5% was obtained from Sigma Aldrich Co.

Single-crystal diffraction measurements were performed at room temperature and high pressures using Huber four-circle diffractometers with Eulerian cradles driven by the *Single* program (Angel *et al.*, 2000). The instrument configurations lead to an FWHM of the individual components of the α_1 - α_2 doublet of the diffracted beams from a quartz single-crystal sample of approximately 0.05–0.07° under hydrostatic conditions. This means that broadening of the peaks due to strain or any other cause is readily detectable. The algorithm used for centering diffraction peaks (Angel *et al.*, 1997) is completed with a final step scan of the ω circle and the resulting profile is fitted with a constrained pair of pseudo-Voigt functions that represent the contribution of the $K\alpha_1$ and $K\alpha_2$ components of the X-ray spectrum (Angel *et al.*, 2000). This refinement procedure provides the peak position of the $K\alpha_1$ component to a precision better than 0.01°, as well as the refined FWHM of the individual components. Each diffracted beam was centered in eight positions on the diffractometer, and the setting angles were determined following the method of King & Finger (1979) to eliminate the effects of diffractometer circle zero offsets, crystal offsets and aberrations in the diffractometer alignment. The reported peak widths at each pressure are the average of the widths refined at each of the eight positions, and the estimated uncertainty is calculated as the standard deviation of these values. We report the width of the 101 reflection throughout, because the (101) planes are oriented parallel to the axis of the diamond-anvil cell. In some measurements a small ruby chip was also included in the DAC to allow pressure to be measured by the fluorescence shift (Mao *et al.*, 1986). In the remaining experiments, pressures were determined from the diffraction pattern of the quartz by using the hydrostatic calibration of its equation of state (Angel *et al.*, 1997).

Gigahertz ultrasonic interferometry was used to determine the onset of shear-wave propagation through the pressure media and thus the glass transition pressures in the neighborhood of 1 GHz of 4:1 methanol-ethanol and 16:3:1 methanol-ethanol-water mixtures. Details of the ultrasonic system are described elsewhere (Jacobsen *et al.*, 2005). Briefly, longitudinal (P) waves are generated at a zinc oxide thin-film transducer, driven by a high-stability radio-frequency (RF) source. Phase-coherent tone bursts 20–50 ns in duration and with adjustable delay are achieved by gating the continuous RF signal with a 5 ns rise-time pulse generator. The P waves are converted to shear (S) waves with a single pure polarization and delivered to the back (table face) of one diamond anvil through mechanical contact with a P-to-S conversion buffer rod (Jacobsen *et al.*, 2004). Shear waves are thus

transmitted through the diamond anvil and, when the media on the far side of the diamond at the culet is fluid, all of the strain energy is back-reflected and detected as a single ‘echo’ (or tone burst) on the 18 GHz broadband sampling oscilloscope. If the media between the acoustic anvil and the opposing anvil supports shear, a second echo from the far culet is observed. The subtle onset of shear-wave propagation through the sample chamber was detected interferometrically, that is, at each pressure, the duration of the input tone burst was extended so as to overlap (in time) with the return of any echo (if present) from the far culet. Then the frequency was scanned between ~ 800 and 1200 MHz and the amplitude of the returning interfered wave was measured as a function of frequency. When the pressure medium supports shear-wave propagation, interference between echoes from the near and far culet cause an interference pattern to develop because they have travelled different distances. The round-trip travel time of shear waves through the media, obtained from the interference spectra, was then combined with the distance between the culets, estimated from micrometre measurements made on the outer (table) facets of the diamonds, to determine the shear-wave velocities. The ultrasonic technique described here is identical to routine travel time experiments through solid mineral samples (Jacobsen *et al.*, 2005), although in this case the sample chamber contains only pressure media. A schematic diagram of the ultrasonic setup is illustrated in Fig. 1, showing how upon transition to a glassy material the pressure medium will support shear waves (at various frequencies), resulting in an echo from the far diamond culet.

3. Results

Each X-ray diffraction measurement was performed after sufficient time to allow the DAC to relax after a pressure change, as indicated by the cessation of shift of the diffraction maxima from the quartz. In the initial experiments, no attempt to heat the cell, nor to cycle the pressure, were made. This procedure thus mimics the normal mode of operation of a DAC for single-crystal diffraction experiments and will provide a practical indication as to the pressures at which the potential for non-hydrostatic behavior of the pressure media should be considered. All of the pressure media studied show a similar pattern of behavior to that illustrated in Fig. 2, which shows the evolution of the width of the rocking curve of quartz in several of the pressure media. Upon initial compression the diffraction peak widths remain constant within experimental uncertainties, and the unit-cell parameters determined from the diffraction peak positions follow the evolution previously reported for hydrostatic conditions (Angel *et al.*, 1997). Above a certain pressure, the peak widths show a continuous increase from those observed at lower pressures. The increase is completely reversible upon subsequent pressure decrease and may thus be assumed to be the result of elastic deformation of the quartz crystal. We define the nominal ‘hydrostatic limit’ of a pressure medium (Table 1) as being the pressure at which a back extrapolation of the peak widths reaches the value observed in the hydrostatic regime. For 2-propanol (Fig. 2) this is ~ 4.2 GPa, in agreement with the previous results (Piermarini *et al.*, 1973) based on changes in the ruby fluorescence

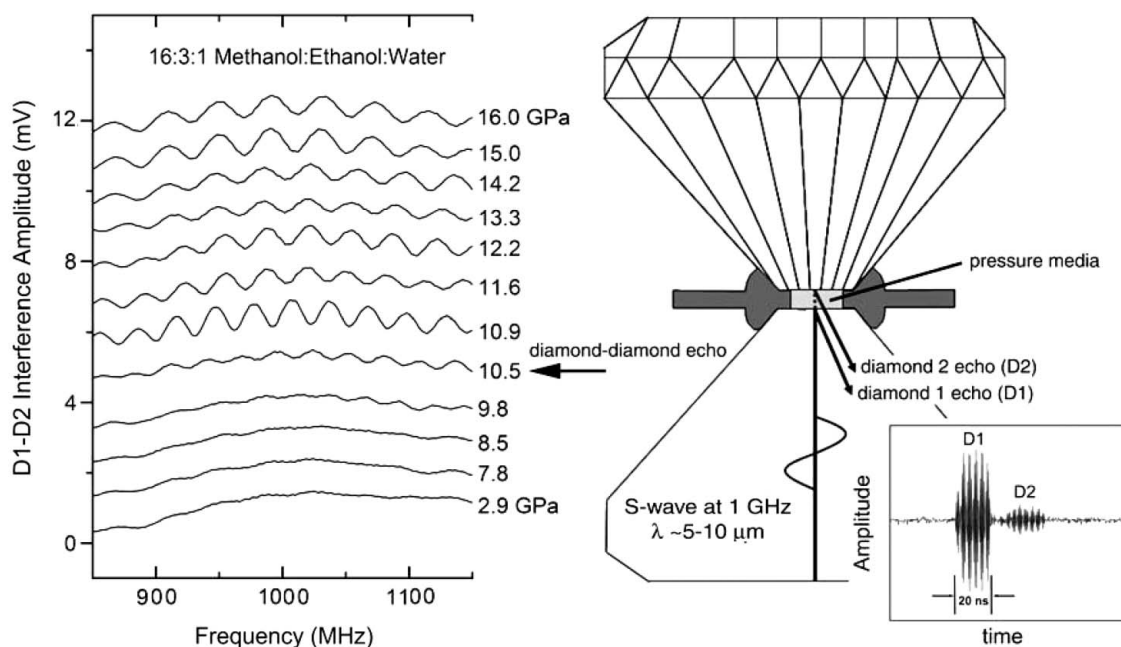


Figure 1 Schematic illustration of the ultrasonic DAC setup (right), illustrating echoes from the acoustic diamond (D1), and the second diamond (D2) for the case when the pressure medium between the culets supports shear strain at 0.8–1.2 GHz. When both D1 and D2 echoes are present and overlapped in time, a frequency scan (left) shows an interference pattern developed from differing path lengths through the sample chamber. For 16:3:1 methanol–ethanol–water (MEW), some interference is observed above 9.8 GPa but only at higher frequencies. Above ~ 10.5 GPa, the medium is glassy across the entire frequency band.

Table 1
Nominal hydrostatic limits of pressure media.

Medium	Hydrostatic limit (GPa)
4:1 Methanol–ethanol	9.8
Anhydrous 2-propanol	4.2
Argon	1.9
Nitrogen	3.0
Glycerol	1.4
Silicone oil, viscosity 0.65 cSt	0.9
Silicone oil, viscosity 37 cSt	0.9

spectra. Similarly, we detect the onset of reflection broadening at ~ 9.8 GPa in the widely used 4:1 methanol–ethanol mixture (Fig. 2). Non-hydrostatic stresses in these alcohols are thus only detected at pressures well in excess of the equilibrium solidus. This has been attributed to difficulties for these compounds to form well organized hydrogen-bonding networks (Brugmans & Vos, 1995; Allan *et al.*, 1998) that would lead to crystallization. Instead, at low pressures the alcohols remain as liquids, which thus can serve as hydrostatic pressure media. The onset of non-hydrostaticity in alcohol pressure media is then associated with a glass transition (Piermarini *et al.*, 1973; Eggert *et al.*, 1992; Grocholski & Jeanloz, 2005). The changes in the shear strengths of these media at their glass transitions appear to be sufficiently great that most experimental methods detect the onset of non-hydrostatic behavior at essentially the same pressure. Thus, for example, we detect broadening of the diffraction maxima from quartz in both 4:1 methanol–ethanol and 2-propanol at the same pressures at which deviations can be detected in the ruby fluorescence spectra and sharp increases are found in the viscosity (Piermarini *et al.*, 1973; Eggert *et al.*, 1992; Grocholski & Jeanloz, 2005).

We detected transmission of GHz-frequency shear waves in 4:1 methanol–ethanol above ~ 9.2 GPa, approximately 0.6 GPa before the onset of peak broadening at 0 Hz, and in 16:3:1 methanol–ethanol–water we detected shear waves

above ~ 10.5 GPa. In both cases, the onset of shear-wave propagation indicates an upper limit that the pressure medium can be considered fluid (hydrostatic) in the 0.8–1.2 GHz range. The difference in transition pressures between the high-frequency and static measurements can result both from the difference in frequency itself, and because the glass will be weaker than the quartz for some pressure interval above the glass transition. Once the glass develops sufficient shear strength the quartz sample will be significantly stressed, and thus broadening of the diffraction maxima will occur. Thus we note that above ~ 10 GPa these glasses are rather stiff, with shear wave velocities at ~ 1 GHz of the order of 3.3 km s^{-1} , based on the measured travel times and estimated thicknesses of the sample chambers (Fig. 3). For comparison, the shear-wave velocity of silica glass and quartz is about $3.7\text{--}3.8 \text{ km s}^{-1}$ at room pressure (McSkimin *et al.*, 1965; Meister *et al.*, 1980). The estimated shear-wave velocity in methanol–ethanol mixtures is in good agreement with bulk sound velocity measurements on pure methanol, which is $\sim 4.5 \text{ km s}^{-1}$ at 1 GHz on the dispersion curve determined by impulsive stimulated scattering (Zaug *et al.*, 1994).

In contrast, both samples of silicone oil of differing viscosities exhibited line broadening at ~ 0.9 GPa, an order of magnitude below the pressures at which an onset of line broadening in the ruby fluorescence signal was previously detected (Ragan *et al.*, 1996; Shen *et al.*, 2004). Glycerol, often used as a non-penetrating pressure medium for the study of meso- and microporous structures (*e.g.* Gatta *et al.*, 2003, 2004), induces broadening of the quartz reflections at ~ 1.4 GPa (Fig. 2). For nitrogen and argon the onset of non-hydrostatic conditions, at least as detected by diffraction line broadening, occurs at pressures slightly above their room-temperature freezing pressures of ~ 1.2 GPa for argon and ~ 2.4 GPa for nitrogen (Fig. 4); we detect broadening at ~ 1.9 GPa in argon and ~ 3 GPa in nitrogen. The onset of line

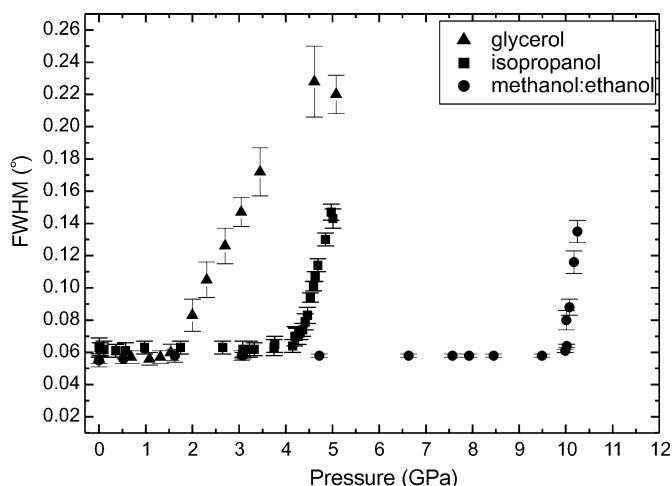


Figure 2
The variation in the widths of the 101 reflection of quartz as a function of nominal pressure in glycerol (triangles), anhydrous 2-propanol (squares) and 4:1 methanol–ethanol (circles).

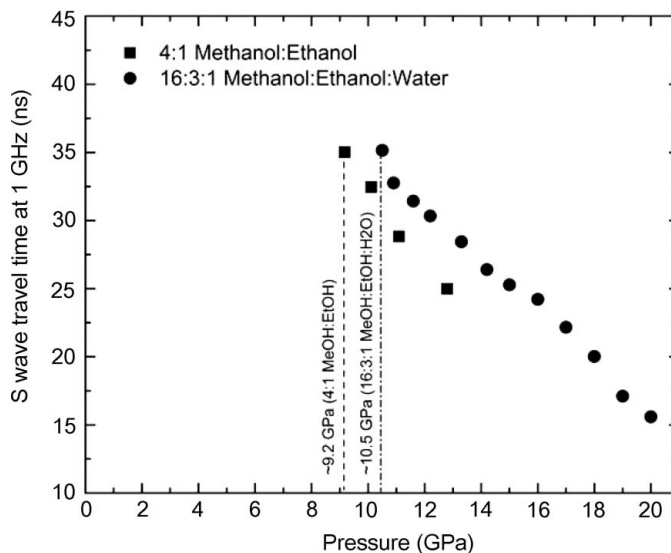


Figure 3
Plot of shear-wave travel times in 4:1 methanol–ethanol (squares) and 16:3:1 methanol–ethanol–water (circles) as a function of pressure above their glass transitions.

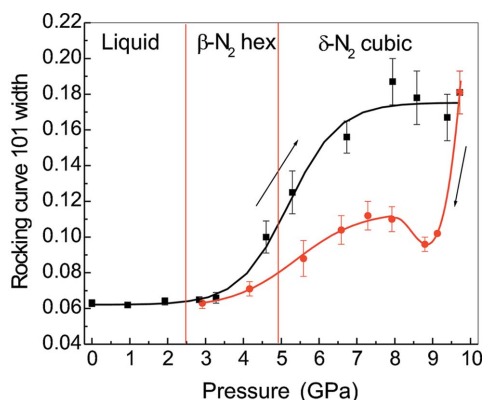


Figure 4
The variation in the widths of the 101 reflection of quartz as a function of nominal pressure in nitrogen.

broadening, and hence the presence of shear stresses in the pressure media, thus occurs at pressures significantly below the oft-quoted hydrostatic limits of ~ 9 GPa for argon (Bell & Mao, 1981) and ~ 13 GPa for nitrogen (Lesar *et al.*, 1979) derived from measurements of ruby fluorescence spectra.

4. Discussion

The stress field in a diamond-anvil cell is normally considered to be axially symmetric and, under non-hydrostatic conditions, the axial stress is higher than the radial stress (Ruoff, 1975; Singh, 2004). The relationship of the broadening of the rocking curve of a single crystal to such a stress field applied by the pressure medium is quite distinct from that for a powder sample. For powders, each diffraction maximum is the composite of many diffraction maxima from many different crystallites within the sample that share the same orientation of their diffraction vector. Differences in the rotation angles of crystallites around this diffraction vector lead to different strains in the various crystallites as a result of the anisotropy of the elastic properties of the crystalline sample as well as grain-to-grain contacts (Singh, 2004). The subsequent analysis of the shift and broadening of diffraction lines is then typically developed by assuming that the entire powder sample is subjected to the same stress field (Ruoff, 1975; Singh, 2004). This is equivalent to the experimental situation of the powder sample only occupying the very center of the gasket hole of a diamond-anvil cell. By contrast, a single crystal is a single coherent object that extends across the sample chamber. It thus collectively samples different stress states simultaneously as a result of the axial and radial stresses decreasing with increasing distance from the axis of the DAC. Our results can be understood, at least qualitatively, in terms of the situation sketched in Fig. 5. If, for convenience of illustration, we label the components of the elastic modulus tensor with respect to the DAC axes and assume that the crystal is axially symmetric as well, then s_{rr} is the component relating the radial strain to the radial stress, and s_{ra} is the off-diagonal component relating the axial stress to radial strain. Under hydrostatic conditions, the axial stress σ_a is equal to the radial stress σ_r , and they are

constant at all positions in the sample chamber. The quartz sample is thus subject to the same stress at all points, and thus exhibits the same radial strain $\epsilon_r = 2\sigma_r s_{rr} + \sigma_a s_{ra}$ at all points in the crystal. Because the radial strain is constant over the entire crystal, the reflections exhibit no broadening. As the pressure is increased into a regime in which the medium has shear strength, a radial gradient in the axial stress is developed across the sample chamber (Meng *et al.*, 1993; Wu & Bassett, 1993). Thus different portions of the quartz crystal experience different stresses σ_a and these result in different portions of the crystal exhibiting different radial strains. The 101 diffraction maxima, from planes oriented with their normals parallel to the radius, will thus be broadened as these planes will have different d -spacings at different distances from the center of the sample chamber. In addition, the coherency of the crystal also contributes to the broadening because the different strains at different radii along a line normal to the diffraction vector (*i.e.* along a line perpendicular to the plane of the diagram in Fig. 5) must result in a curvature of the planes. For this reason it is not possible to extract a measure of the overall range of differential strain, and thus the stress gradients in the pressure media, from a measurement of the widths of the diffraction peaks.

As pressure is increased further, the stress gradient increases and this gives rise to the observed increased broadening of reflections (Fig. 2). In some pressure media, a plateau is found in the widths of the rocking curves above a certain pressure, as illustrated for nitrogen in Fig. 4. We suggest that this plateau regime corresponds to the maximum stress gradient that can be supported by the pressure medium, which is a measure of the yield stress of the medium at room temperature (Ruoff, 1975). Although further pressure increase may thus lead to higher stress gradients, these are relaxed by flow in the pressure medium until the stress gradient falls back to that supported by the shear strength of the media, prior to the diffraction measurement.

Some further observations have been made of the quartz crystal loaded with nitrogen as pressure medium. If the entire

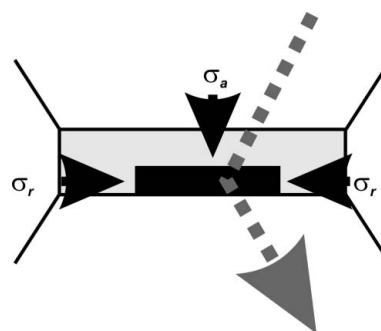


Figure 5
A diagrammatic cross section of a DAC loaded with a single crystal, indicating the stress state in the pressure medium. Under hydrostatic conditions, the axial stress σ_a is equal to the radial stress σ_r , and they are constant at all positions within the sample chamber. Under non-hydrostatic conditions, both vary as a function of distance from the center of the sample chamber, but the stress field is assumed to remain axially symmetric. The path of X-rays through the cell when set for a 101 reflection from quartz in our experiments is indicated by the dashed line.

cell is heated to a temperature below the melting point of the medium, the peak widths of the quartz initially decrease with time, but do not return to the hydrostatic, unstrained value. Of course, heating any pressure medium above its melting point at pressure will allow hydrostatic conditions to be recovered, but this is not always practical. However, even after the melting of the pressure medium, the absence of shear stress cannot be guaranteed upon cooling it back into the solid phase. Furthermore, if pressure is decreased once the plateau regime in line broadening is reached the widths of the quartz lines were found to drop rapidly to values significantly below those found on pressure increase. This suggests that pressure cycling might be used to reduce the stress state on the sample without the need for heating, although hydrostatic conditions will not be achieved by this method. As a corollary we note that the stress state of a sample in a non-hydrostatic pressure medium clearly depends on its history of pressure increase and cycling, including the rate at which pressure is increased (Piermarini *et al.*, 1973; Besson & Pinceaux, 1979).

5. Conclusions

Except for the alcohols in which the onset of non-hydrostatic behavior is associated with a glass transition, the hydrostatic pressure limits listed in Table 1 are, in most cases, significantly lower than the values often quoted in the literature. Nonetheless, they should be considered the maximum pressures to which each pressure medium may be hydrostatic. For at least two important reasons we must emphasize that our measurements do not guarantee that these pressure media do not have shear strength and thus do not support shear stresses at lower pressures. First, were we to use a softer crystal or more sensitive measurement technique to probe the properties of the pressure media, it is quite possible that shear stresses might be detected at lower nominal pressures. Second, for media such as alcohols in which the onset of non-hydrostatic behavior is associated with a glass transition, we have shown that the glass transition pressure is frequency-dependent and is lower at higher frequencies, in the same way that the glass transition temperature increases with frequency at room pressures. Thus, we find that the 4:1 methanol–ethanol mixture supports the propagation of gigahertz-frequency shear waves at 9.2 GPa (Figs. 1 and 3), whereas static measurements indicate the 0 Hz glass transition pressure is between 9.8 and 10.8 GPa (this work; Piermarini *et al.*, 1973; Eggert *et al.*, 1992; Grocholski & Jeanloz, 2005). Further evidence for this frequency dependence can be observed in Fig. 1, which shows that the 4:1 methanol–ethanol mixture supports shear only above ~ 1 GHz at 9.8 GPa, but over the entire bandwidth at pressure in excess of ~ 10.5 GPa.

This work was supported by the NSF in the form of grants EAR-0408460 to Nancy Ross and RJA. SDJ was supported in part by NSF EAR-0440112, a fellowship from the Carnegie Institution of Washington and the Carnegie/DOE Alliance Center. The North Atlantic Treaty Organization supported

MB with a grant and fellowship (DGE-0410297). GDG thanks the Bayerisches Geoinstitut (University of Bayreuth, Germany) where the experiment on glycerol was performed, and the Società Italiana di Mineralogia e Petrologia and acknowledges the support of NSF Grant EAR-0229472 to Nancy Ross for his research visit to Virginia Tech. Virginia Tech provided funds for the purchase of the Huber diffractometer. Ruby pressure measurements were conducted with the Raman system in the Vibrational Spectroscopy Laboratory in the Department of Geosciences at Virginia Tech.

References

- Allan, D. R., Clark, S. J., Brugmans, M. J. P., Ackland, G. J. & Vos, W. L. (1998). *Phys. Rev. B*, **58**, R11809–R11812.
- Allan, D. R., Clarke, S. J., Dawson, A., McGregor, P. A. & Parsons, S. (2002). *Acta Cryst.* **B58**, 1018–1024.
- Angel, R. J. (1997). *Am. Mineral.* **82**, 836–839.
- Angel, R. J., Allan, D. R., Miletich, R. & Finger, L. W. (1997). *J. Appl. Cryst.* **30**, 461–466.
- Angel, R. J., Downs, R. T. & Finger, L. W. (2000). *Rev. Mineral. Geochem.* **41**, 559–596.
- Bell, P. M. & Mao, H. K. (1981). *Annual Report of the Director, Geophysical Laboratory*, Vol. 80, pp. 404–406. Carnegie Institution of Washington.
- Besson, J. M. & Pinceaux, J. P. (1979). *Rev. Sci. Instrum.* **50**, 541–543.
- Boldyreva, E. V., Shakhtshneider, T. P., Ahsbabs, H., Sowa, H. & Uchtmann, H. (2002). *J. Therm. Anal. Calorim.* **68**, 437–452.
- Brugmans, M. J. P. & Vos, W. L. (1995). *J. Chem. Phys.* **103**, 2661–2669.
- Bujak, M. & Angel, R. J. (2006). *J. Phys. Chem. B*, **110**, 10322–10331.
- Chai, M. & Brown, J. M. (1996). *Geophys. Res. Lett.* **23**, 3539–3542.
- Decker, D. L., Petersen, S., Debray, D. & Lambert, M. (1979). *Phys. Rev. B*, **19**, 3552–3555.
- Eggert, J. H., Xu, L. W., Che, R. Z., Chen, L. C. & Wang, J. F. (1992). *J. Appl. Phys.* **72**, 2453–2461.
- Forman, R. A., Piermarini, G. J., Barnett, J. D. & Block, S. (1972). *Science*, **176**, 284–285.
- Gatta, G. D., Boffa-Ballaran, T., Comodi, P. & Zanazzi, P. F. (2004). *Am. Mineral.* **89**, 633–639.
- Gatta, G. D., Comodi, P. & Zanazzi, P. F. (2003). *Microporous Mesoporous Mater.* **61**, 105–111.
- Grocholski, B. & Jeanloz, R. (2005). *J. Chem. Phys.* **123**, 204503(1–6).
- Haines, J., Léger, J. M., Gorelli, F. & Hanfland, M. (2001). *Phys. Rev. Lett.* **87**, 15503.
- Hazen, R. M. (1983). *Science*, **219**, 1065–1067.
- Hazen, R. M. & Finger, L. W. (1984). *J. Appl. Phys.* **56**, 1838–1840.
- Jacobsen, S. D., Reichmann, H. J., Kantor, A. & Spetzler, H. (2005). *Advances in High-Pressure Technology for Geophysical Applications*, edited by J. Chen, Y. Wang, T. S. Duffy, G. Shen & L. Dobrzynetskaia, *A Gigahertz Ultrasonic Interferometer for the Diamond Anvil Cell and High-Pressure Elasticity of Some Iron-Oxide Minerals*, pp. 25–48. Amsterdam: Elsevier.
- Jacobsen, S. D., Spetzler, H., Reichmann, H. J. & Smyth, J. R. (2004). *Proc. Natl Acad. Sci. USA*, **101**, 5867–5871.
- Kenichi, T. (1999). *Phys. Rev. B*, **60**, 6171–6174.
- Kim-Zajonz, J., Werner, S. & Schulz, H. (1999). *Z. Kristallogr.* **214**, 331–336.
- King, H. & Finger, L. W. (1979). *J. Appl. Cryst.* **12**, 374–378.
- Lee, Y., Vogt, T., Hriljac, J. A., Parise, J. B., Hanson, J. C. & Kim, S. J. (2002). *Nature (London)*, **420**, 485–489.
- Lesar, R., Ekberg, S. A., Jones, L. H., Mills, R. L., Schwalbe, L. A. & Schiferl, D. (1979). *Solid State Commun.* **32**, 131–134.
- Machon, D., Dmitriev, V. P., Bouvier, P., Timonin, P. N., Shirokov, V. B. & Weber, H.-P. (2003). *Phys. Rev. B*, **68**, 144104.

- McSkimin, H. J., Andreacht, P. & Thurston, R. N. (1965). *J. Appl. Phys.* **36**, 1624–1632.
- Mao, H. K., Xu, J. & Bell, P. M. (1986). *J. Geophys. Res.* **B91**, 4673–4676.
- Meister, R., Robertson, E. C., Were, R. W. & Raspert, R. (1980). *J. Geophys. Res.* **85**, 6461–6470.
- Meng, Y., Weidner, D. J. & Fei, Y. (1993). *Geophys. Res. Lett.* **20**, 1147–1150.
- Piermarini, G. J., Block, S. & Barnett, J. D. (1973). *J. Appl. Phys.* **44**, 5377–5382.
- Ragan, D. D., Clarke, D. R. & Schiferl, D. (1996). *Rev. Sci. Instrum.* **67**, 494–496.
- Resel, R., Oehzelt, M., Shimizu, K., Nakayama, A. & Takemura, K. (2004). *Solid State Commun.* **129**, 103–106.
- Richet, P., Xu, J. A. & Mao, H. K. (1988). *Phys. Chem. Miner.* **16**, 207–211.
- Ruoff, A. L. (1975). *J. Appl. Phys.* **46**, 1389–1392.
- Sharma, S. M. & Gupta, Y. M. (1991). *Phys. Rev. B*, **43**, 879–893.
- Shen, Y., Kumar, R. S., Pravica, M. & Nicol, M. F. (2004). *Rev. Sci. Instrum.* **75**, 4450–4454.
- Sidorov, V. A. & Sadykov, R. A. (2005). *J. Phys. Condens. Matter*, **17**, S3005–S3008.
- Singh, A. K. (2004). *J. Phys. Chem. Solids*, **65**, 1589–1596.
- Varga, T., Wilkinson, A. P. & Angel, R. J. (2003). *Rev. Sci. Instrum.* **74**, 4564–4566.
- Wu, T.-C. & Bassett, W. A. (1993). *Pure Appl. Geophys.* **141**, 509–519.
- Zaug, J. M., Slutsky, L. J. & Brown, J. M. (1994). *J. Phys. Chem.* **98**, 6008–6016.